

Tri-FusionNet: Enhancing Image Description Generation with Transformer-based Fusion Network and Dual Attention Mechanism

Lakshita Agarwal*, Bindu Verma[†] * Department of Information Technology, Delhi Technological University, Delhi, India - 110042 [†] Assistant Professor, Department of Information Technology, Delhi Technological University, Delhi, India - 110042

Abstract—Image description generation is essential for accessibility and AI understanding of visual content. Recent advancements in deep learning have significantly improved natural language processing and computer vision. In this work, we propose Tri-FusionNet, a novel image description generation model that integrates transformer modules: a Vision Transformer (ViT) encoder module with dual-attention mechanism, a Robustly Optimized BERT Approach (RoBERTa) decoder module, and a Contrastive Language-Image Pre-Training (CLIP) integrating module. The ViT encoder, enhanced with dual attention, focuses on relevant spatial regions and linguistic context, improving image feature extraction. The RoBERTa decoder is employed to generate precise textual descriptions. CLIP’s integrating module aligns visual and textual data through contrastive learning, ensuring effective combination of both modalities. This fusion of ViT, RoBERTa, and CLIP, along with dual attention, enables the model to produce more accurate, contextually rich, and flexible descriptions. The proposed framework demonstrated competitive performance on the Flickr30k and Flickr8k datasets, with BLEU scores ranging from 0.767 to 0.456 and 0.784 to 0.479, CIDEr scores of 1.679 and 1.483, METEOR scores of 0.478 and 0.358, and ROUGE-L scores of 0.567 and 0.789, respectively. On MS-COCO, the framework obtained BLEU scores of 0.893 (B-1), 0.821 (B-2), 0.794 (B-3), and 0.725 (B-4). The results demonstrate the effectiveness of Tri-FusionNet in generating high-quality image descriptions.

Index Terms—Image Description Generation, Natural Language Processing, Computer Vision, Transformers, Dual Attention Mechanism, Artificial Intelligence.

I. INTRODUCTION

IN order to improve accessibility and comprehension, image description generation, which is essential to computer vision and artificial intelligence— involves producing textual descriptions of images. These descriptions, which make use of transformer architectures and deep learning, seek to accurately capture the context and content of images [1]. By combining computer vision and natural language processing, this multi-modal method allows machines to understand and communicate with visual content in a way that is similar to that of humans. The goal of the research is to find image-processing algorithms that efficiently link textual and visual elements while preserving linguistic fluency. Applications include social media image annotation, real-time navigation systems, visual question answering, helping the blind, and self-driving automobiles. After breakthroughs in image classification models,

adversarial examples are being developed for more complex tasks like image description generation [2].

Transformer models excel in generating image descriptions using self-attention but struggle with complex relationships. Single transformers may fail to capture both global and local details, while dual models often struggle to integrate visual and textual information effectively. This can hinder fine-grained visual understanding and complicate non-auto-regressive techniques [3]. To address these issues, we propose a model combining Vision Transformer (ViT) with dual attention, RoBERTa, and a CLIP integration module. ViT transforms images into embedding sequences, capturing global and local features through transformer layers and pre-training on large datasets for image classification. RoBERTa, based on BERT, enhances textual context understanding by leveraging extensive text pre-training [4]. CLIP, developed by OpenAI, enables vision-language learning by aligning image and text representations for multimodal tasks [5].

With dual attention, the suggested Tri-FusionNet architecture combines three transformers to improve image descriptions by making them more contextually relevant and advanced. This fusion includes a CLIP integrating model for textual representation generation, a RoBERTa decoder for category derivation and a Vision Transformer (ViT) for feature capture. By combining ViT, RoBERTa and CLIP with dual attention, one may enhance the quality of descriptions and build a robust and flexible system for producing visual descriptions.

The major contribution of the proposed framework is highlighted below:

- This work presents a novel image description-generating model called Tri-FusionNet, which represents a major breakthrough in multi-modal approaches to generating precise and contextually rich descriptions. This method improves the model’s fine-tuning capabilities by combining several components, which increases the efficacy of creating image descriptions.
- The combination of ViT encoder with dual-attention, RoBERTa decoder, and CLIP integration module is employed to create an efficient model that maximizes the interaction between different modalities, resulting in more accurate and contextually appropriate image descriptions.
- The proposed framework addresses the challenges posed by different benchmark datasets by developing a model

that can adapt to the characteristics of each dataset as well as potentially setting new state-of-the-art results on these datasets.

Organization of the paper is as follows: Section II explores prior research and previous works. Section III provides a comprehensive presentation of the suggested framework. Section IV presents and analyses the experimental design, benchmark dataset information, results and ablation study. Section V provides a conclusion as well as a discussion of the ability of the study and its future directions.

II. RELATED WORK

Deep learning frameworks have been investigated for autonomous image description systems. These frameworks are extensively used in the fields of computer vision and human-computer interaction. The transformer exhibits potential for multi-modal tasks such as visual description creation, as it is skilled at collecting long-range dependencies and modeling sequential data. Li et al. [6] developed the EnTangled Attention (ETA) Transformer, exhibiting state-of-the-art performance on the MSCOCO dataset, whereas Cornia et al. [7] presented M2, a Meshed Transformer with Memory, for image description generation. Furthermore, a Multi-modal Transformer (MT) model was introduced by Yu et al. [8], that stores intra-modal and inter-modal interactions in a single attention block, enabling precise description development and sophisticated multi-modal reasoning.

Radford et al. [9] demonstrated that pre-training a model to predict image-caption pairs from a dataset of 400 million (image, text) pairs enables zero-shot transfer to various downstream tasks, achieving competitive performance without task-specific training. MiniGPT-v2 is a unified model designed to handle diverse vision-language tasks like image description, visual question answering, and visual grounding, using unique task identifiers to improve learning efficiency and performance on various benchmarks [10]. In order to improve image captioning performance on the MS COCO and Flickr8k datasets, Yang et al. [11] suggested SAMT-Generator, a multi-stage transformer feature enhancement network with second attention and Maxout decoding. A novel approach of the S^2 transformer was developed that integrated Spatial-aware Pseudo-supervised and Scale-wise Reinforcement modules, achieving state-of-the-art results on the MSCOCO benchmark [12]. Yang et al. [13] presented a fully Transformer-based image captioning model called CA-Captioner, which applies HAPE positional encoding, LSM, RNorm function, and LFE, thereby achieving improved performance on the MS COCO, Flickr8k, and Flickr30k datasets, especially in terms of BLEU4 and CIDEr metrics.

On the Flickr30k and MSCOCO datasets, Parvin et al. [14] proposed a double-attention framework that outperformed state-of-the-art models. By utilising previous activations to improve semantic attention and performance, PMA-Net [15] integrates prototypical memory vectors into Transformer-based image captioning, attaining a 3.7 CIDEr boost on the COCO dataset. By treating heterogeneous encodings (such as visual and textual) as augmented views and using a shared encoder

with contrastive loss to improve representation quality and a hierarchical decoder to adaptively weigh views, HAAV [16] presents a novel method for image captioning. It achieves notable CIDEr improvements on MS-COCO (+5.6%) and Flickr30k (+16.8% with SSL) datasets. DualVision Transformer (Dual-ViT) was introduced by Yao et al. [17], providing higher accuracy with effective token vector compression. Spatial Pyramid Transformer (SPT) was mainly used for adaptive semantic interaction across grid resolutions, preserving spatial and fine-grained information, achieving state-of-the-art performance on MS-COCO [18] for image description generation.

The challenges of creating image descriptions remain, despite the progress made in medical imaging and NLP with models such as ETA Transformer, Multi-modal Transformer (MT) and Dual-Level Collaborative Transformer (DLCT). These challenges include the semantic gap between language and vision, as well as the absence of global information that is critical for scene comprehension. The suggested Tri-FusionNet combines dual attention, RoBERTa and CLIP transformers with Vision Transformer (ViT) to address these issues. By using ViT for image embedding, RoBERTa for textual interpretation, and CLIP for visual-textual fusion, it is possible to improve understanding of visual content.

III. PROPOSED FRAMEWORK

Recently, image description creation has gained a lot of attention as a challenging topic combining computer vision and natural language processing (NLP). Although the current models have come a long way, there is still an opportunity for development in producing precise and contextually appropriate descriptions. This work presents Tri-FusionNet, which combines a dual attention mechanism with Vision Transformer (ViT), CLIP, and RoBERTa decoder to improve spatial and channel-wise information extraction from images. Better descriptive words are generated over a range of images, advancing image description generation. The model is optimized with Adam optimizer and Cross-Entropy loss over epochs. Its performance is assessed using metrics including BLEU, CIDEr, ROUGE-L, and METEOR scores on benchmark datasets. Figure 1 represents the framework of the proposed approach.

A. Overview of the Proposed Architecture:

1) *Data Pre-processing*: The data preprocessing step in the proposed Tri-FusionNet framework involves normalizing the input images' pixel values to enhance the model's performance. The mean and standard deviation of the pixel values throughout the dataset are computed to accomplish this. The distribution of the pixel values is then altered to have a standard deviation (or variance) of one and a mean of zero. This normalization process reduces the effect of varied lighting or contrasts between images by standardizing the range of pixel values. The model can learn more from the data by focusing the values around zero and scaling them to have unit variance, guaranteeing that each feature contributes equally to the training process. Figure 1(a) demonstrates the Data Pre-Processing step. Next, to prepare the data for the Vision Transformer (ViT) encoder module in image description generation,

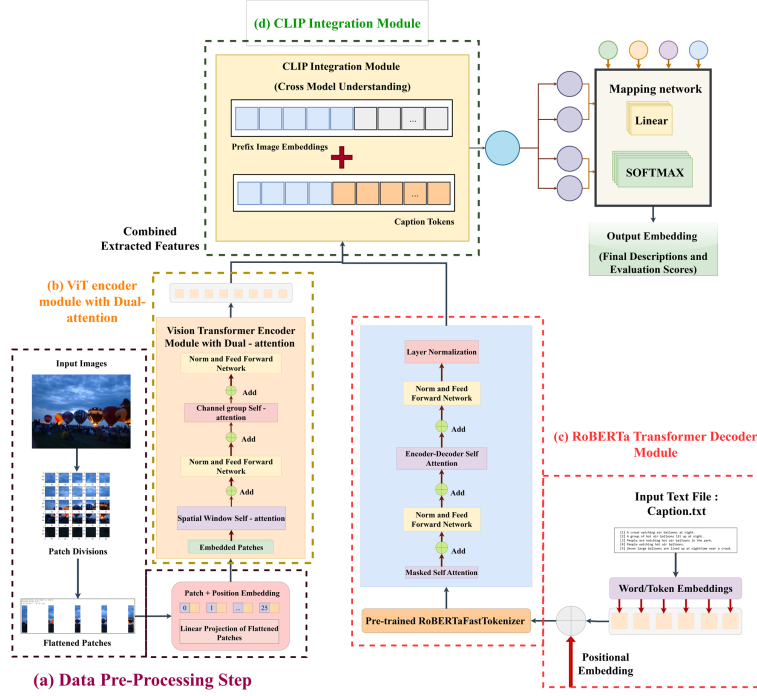


Fig. 1. Structural representation of Tri-FusionNet framework: The architecture consists of three phases: firstly, high-level visual features are first extracted from pre-processed images using a Vision transformer encoder with dual-attention mechanism; next, words from the input caption file are tokenized by a RoBERTa decoder; and last, the combined data is fed into a CLIP-integrating module to create image descriptions using dense network layers.

input images are divided into fixed-size patches. To construct embeddings, each patch is flattened and projected linearly. The process of patch extraction and positional encoding is thoroughly explained in the `supplementary.tex` file. The ViT encoder receives sequences of tokenized patches that have been enhanced with positional data. Through this procedure, the model is able to efficiently collect the image’s spatial and visual properties, which sets the stage for the next tasks, like labeling the image.

2) *Vision Transformer Encoder Module with Dual Attention Mechanism*: The input image is divided into fixed-size patches using the Vision Transformer’s encoder-based architecture, which is then processed through transformer layers and linearly embedded. Its ability to retrieve relevant data from both spatial and channel-wise dimensions is enhanced by the dual-attention process, which makes accurate descriptions possible. In the vision transformer encoder with a dual attention mechanism, we adopt a hierarchical layout. The encoder combines spatial window attention with channel-group attention and is structured into four phases: (a) insertion of the patch embedding layer, (b) application of spatial window attention, (c) utilization of channel-group attention, and (d) incorporation of the jointly extracted features. Figure 1(b) demonstrates the Vision encoder module with dual-attention mechanism. In the initialization phase, the input is in the form of patches along with positional embedding obtained from the data pre-processing stage. Assuming a visual feature R with dimensions $R^{(P \times C)}$, where P represents the total number of patches and C is the total number of channels, the standard global self-

attention is represented by Equation (1):

$$S_A(Q, K, V) = \text{Concat}(\text{head}_1, \dots, \text{head}_{N_h}), \quad (1)$$

where,

$$\text{head}_i = \text{Attention}(Q_i, K_i, V_i) = \text{Softmax}\left(\frac{Q_i K_i^T}{\sqrt{C_h}}\right) V_i \quad (2)$$

here, $Q_i = X_i \times (W_i)^Q$, $K_i = X_i \times (W_i)^K$ and $V_i = X_i \times (W_i)^V$. Consider $R^{P \times C_h}$ dimensional visual features with N_h heads, where X_i represents the i th head of the input feature and W_i denotes the projection weights for the i th head in the context of Q, K, V , with $C = C_h \times N_h$.

The model concurrently arranges spatial window attention and channel group attention in the vision transformer with a dual attention mechanism to obtain both local and global data but with a linear complication to the spatial dimension. The spatial window attention algorithm calculates self-attention within local windows, which are positioned to equally and non-overlapping segments in the field of vision. Assuming the presence of N_w distinct windows, each comprised of P_w patches, the total number of patches, denoted as P , can be expressed as $P = P_w \times N_w$. The representation of spatial window attention is given by Equation (3):

$$\text{Attention}_w(Q, K, V) = (\text{Attention}(Q_i, K_i, V_i))^{N_w} \quad i = 0 \quad (3)$$

where each $Q_i, K_i, V_i \in \mathbb{R}^{P_w \times C_h}$ are local window queries, keys, and values, respectively, and P is the spatial size presenting the linear complexity.

An alternative viewpoint on self-attention is provided by channel-wise attention, which ensures thorough spatial domain coverage by concentrating on tokens at the patch level as

opposed to pixels. Each transposed token, with the number of heads set to 1, engages with global data in a linear spatial complexity along the channel dimension. $C = N_g \times C_g$ is the outcome of letting C_g represent the number of channels in each group and N_g the number of groups. As a result, Equation (4) defines global channel group attention, which allows tokens at the image level to interact across channels.

$$\text{Attention}_c(Q, K, V) = \left(\left(\text{Attention}_{\text{group}}(Q_i, K_i, V_i) \right)^T \right)_{i=0}^{N_g} \quad (4)$$

where, every $Q_i, K_i, V_i \in \mathbb{R}^{P \times C_g}$ represents grouped channel-wise image-level queries, keys and values.

The final encoder output of the Vision Transformer using the dual attention mechanism can be represented by Equation (5):

$$E_{\text{output}} = \text{Concat}(\text{Attention}_w(Q, K, V), \text{Attention}_c(Q, K, V)) \quad (5)$$

$\text{Attention}_w(Q, K, V)$ represents the spatial window attention and $\text{Attention}_c(Q, K, V)$ represents the channel group attention, as defined in Equations (3) and (4), respectively. In order to achieve linear complexity in both dimensions for computational efficiency, the final encoder output combines channel group attention and spatial window attention. In contrast to spatial-wise global attention, channel attention functions globally, aggregating information rather than locally. It is a complement to spatial window attention. By distributing weights according to how relevant they are to the task, the model uses its attention mechanism to prioritize particular image patches. By using these weights, heat maps are produced that show the areas of the image where the model focuses. On the heat map, places that are important for accurate and contextually rich descriptions are indicated by intense areas.

3) *RoBERTa Decoder*: The study presents a novel approach to image description generation that combines natural language processing (NLP) and computer vision. A Vision Transformer (ViT) with dual attention is employed to extract visual information. Simultaneously, textual data from a "caption.txt" file is used during training to build word embeddings and guide the model in learning semantic relationships between images and their descriptions. This process helps optimize the model and align visual and textual features effectively. During inference, the model does not require an input description or text file. Instead, it generates a new description based solely on the visual features extracted from the input image. This distinction ensures the model's flexibility and generalization, enabling it to produce unique and contextually rich descriptions for each image. These embeddings are seamlessly integrated into a decoder model based on RoBERTa, an enhanced version of BERT, along with ViT-extracted image features. Figure 1(c) demonstrates the step involved in the RoBERTa decoder module.

The decoder uses RoBERTa's pre-trained language understanding abilities to contextualize the data from the text and image embedding, allowing it to produce descriptions that generate better explanations and are relevant to the context. To decode and generate image descriptions, the RoBERTa decoder module is obtained from the following Equation (6).

$$D_{\text{Output}} = \text{RoBERTaDecoder}(W_{\text{emb}}, C), \quad (6)$$

where, W_{emb} represents the word embeddings generated from the caption data, C is the additional contextual information derived from the original caption file, and D_{Output} is the output generated by the RoBERTa decoder, which consists of the final description of the image. Through multiple layers of feed-forward neural networks and self-attention, multiple word embeddings are processed by the RoBERTa decoder, which enables it to efficiently contextualize the textual information.

4) *CLIP Integration Module*: The final step of the proposed approach involves generating image embeddings using a Vision Transformer (ViT) with a dual attention mechanism and text embeddings using the RoBERTa decoder. This integration aims to combine the ViT encoder, RoBERTa decoder, and CLIP for effective image description generation. During the embedding generation process, the ViT encoder is used to obtain image embeddings from the image dataset, while the RoBERTa decoder generates text embeddings from the caption data. The joint representation of the image and its corresponding text is then obtained by aligning these embeddings in the subsequent phase. Specifically, CLIP's encoder is used to align the visual and textual embeddings through contrastive learning, ensuring that the visual and textual features are mapped into a shared space for accurate description generation. The embeddings obtained from both the ViT encoder and the RoBERTa decoder are concatenated to form a unified representation, as shown in Equation (7):

$$CLIP_{\text{integration}} = \text{Concatenate}(E_{\text{output}}, D_{\text{output}}), \quad (7)$$

where E_{output} is the image embedding from the ViT encoder, D_{output} is the text embedding from the RoBERTa decoder, and $CLIP_{\text{integration}}$ represents the combined embedding used by the CLIP model. This integrated representation helps generate coherent and accurate image descriptions by aligning the visual and textual information effectively. The model uses a contrastive loss function in the embedding space to distinguish between positive and negative pairs, ensuring the alignment between visual and textual features. The final integration module, after encoding and decoding the image-description pair, generates the output descriptions. The architectural explanation of the CLIP integration module is explained in the `supplementary.txt` file.

The reference file for descriptions is crucial in assessing how well the Tri-FusionNet model generates descriptions. Visual features extracted from images are projected into a higher-dimensional space using a linear layer, allowing the model to capture intricate relationships among input features. These features are then normalized into a probability distribution across the lexicon of possible words or tokens using a Softmax layer. During training and evaluation, the model generates predicted descriptions, which are compared to reference descriptions using evaluation metrics such as CIDEr, ROUGE-L, BLEU 1-4, and METEOR to assess the model's ability to capture and translate context and image semantics into accurate descriptions.

The Tri-FusionNet model operates through a synergistic pipeline. The Vision Transformer (ViT) encoder with dual attention, RoBERTa decoder, and CLIP integration module

collaborate to generate accurate and contextually rich image captions.

- To handle input images, the Vision Transformer (ViT) encoder flattens, divides them into patches, and embeds positional encodings. Its dual attention method combines Spatial Window Self-Attention, which concentrates on local spatial relationships to maintain contextual importance, with Channel Group Self-Attention, which catches fine-grained features inside image channels. As a result, both local details and global context are successfully represented in the rich visual feature embeddings.
- To process the input text file with ground truth descriptions, the RoBERTa decoder tokenises the text, embeds the tokens, then decodes them into contextual embeddings. It uses its pre-trained language understanding to ensure fluency and coherence and Masked Self-Attention to concentrate on sequentially relevant tokens. This produces textual embeddings that effectively express the descriptions’ semantic meaning and linguistic structure.
- Using a contrastive learning technique, the CLIP integration module maps both modalities into a common latent space by aligning textual embeddings from the RoBERTa decoder and visual features from the ViT encoder. By facilitating cross-modal fusion and preserving semantic coherence, this alignment makes it possible to produce linguistically correct and visually justified descriptions.

The model optimizes for metrics such as BLEU, CIDEr, METEOR, and ROUGE-L and provides accurate and contextually rich descriptions through parallel processing, dual attention, and contrastive learning. By utilizing each module’s unique capabilities to convert raw image and text inputs, the approach guarantees high-quality description generation. The detailed algorithm of the proposed model is given in the `supplementary.tex` file.

IV. EXPERIMENTAL ANALYSIS

The proposed model was evaluated using Google Colab Pro+ with 52 GB RAM, an NVIDIA A100 GPU (40 GB VRAM), and a virtual Intel Xeon CPU. Implemented in Keras and TensorFlow 2.12, Tri-FusionNet integrates three transformer modules, increasing computational demands. Optimization techniques like parallelization, mixed precision training, and resource management reduce memory usage and ensure efficiency. Despite its complexity, model parallelism enables viability on limited hardware. Scalability tests on larger datasets showed a linear increase in training time, demonstrating efficient scaling. Optimized attention mechanisms and parameter sharing enhance computational efficiency compared to state-of-the-art models, balancing performance with resource constraints. The model was tested on MSCOCO¹, Flickr8k², and Flickr30k³, with efficiency, cost, and scalability compared in Table I.

Because of its transformer and CLIP components, the proposed Tri-FusionNet model has a moderate processing cost

¹<https://github.com/cocodataset/cocoapi>

²<https://www.kaggle.com/adityajn105/flickr8k>

³<https://www.kaggle.com/hsankesara/flickr-image-dataset>

TABLE I
COMPARISON OF TRI-FUSIONNET WITH STATE-OF-THE-ART MODELS ON SCALABILITY AND COMPUTATIONAL COST.

Model	Architecture	Scalability	Computational Cost	Efficiency
NIC [19]	CNN with Attention Mechanism	Limited scalability	Low cost and less resource-intensive	Good for smaller tasks but lacks richness
BLIP Transformer [20]	Vision-Language Pretraining	Scales well with efficient pretraining	Moderate cost and compact architecture	Balanced performance and cost
M2 Transformer [7]	Memory-Augmented Transformer	Effective for mid-sized datasets	Moderate cost and memory-efficient	Competitive with moderate resources
Tri-FusionNet	ViT, RoBERTa, CLIP	Handles large datasets	Moderate cost and memory efficient	Superior image-text alignment

but excels at handling huge datasets. On the other hand, BLIP Transformer [20] provides a fair trade-off between cost and performance, whereas models such as NIC [19] and M2 Transformer [7] are more resource-efficient but less scalable.

The implementation details of the proposed framework is demonstrated thoroughly in `supplementary.tex` file.

A. Ablation Study:

An ablation study was carried out in order to fully comprehend the contributions of each element in the suggested image description generation model. The objective of this study is to assess the impact of the proposed Tri-FusionNet model, which integrates the CLIP model, RoBERTa and Vision Transformer (ViT) with dual attention, on the overall performance. Through heat map analysis, the model can learn more about how it interprets visual cues and focuses on various areas of the image. This comprehension can enhance the model’s architecture, boost its functionality, and make the model’s decision-making process more interpretable, as shown in Figure 2.



Fig. 2. Example of obtained heat maps based on dual-attention mechanism.

A thorough study of the outcomes within the framework of the work proposed for MSCOCO dataset is shown in Table II. It presents various results of evaluation metrics for different models applied to the input image dataset.

The Tri-FusionNet model sets a new benchmark by significantly outperforming baseline models among those evaluated on the MSCOCO dataset for image description generation, including the CNN-RNN Model, CNN-LSTM Model, ViT with Attention, ViT with Dual Attention, Vanilla ViT, ViT only, RoBERTa Transformer, CLIP Transformer, and ViT with RoBERTa Model. It achieves a 1.88 CIDEr score increase and notable BLEU values (0.893, 0.821, 0.794, and 0.725). Tri-FusionNet also demonstrates better precision, recall, and alignment with reference phrases, along with enhanced n-gram

TABLE II
PERFORMANCE METRICS OF IMAGE DESCRIPTION GENERATION MODELS
IN THE MSCOCO DATASET

Model	B-1	B-2	B-3	B-4	C	M	R-L
CNN-RNN Model	0.54	0.45	0.33	0.21	1.02	0.31	0.27
CNN-LSTM Model	0.55	0.42	0.30	0.28	1.20	0.48	0.35
ViT with Attention	0.57	0.45	0.34	0.29	1.05	0.40	0.39
ViT with Dual Attention	0.61	0.50	0.38	0.27	1.52	0.43	0.31
Vanilla ViT	0.72	0.61	0.50	0.38	1.45	0.52	0.45
ViT Only	0.62	0.56	0.42	0.34	0.785	0.44	0.39
RoBERTa Transformer	0.73	0.68	0.51	0.43	1.54	0.62	0.50
CLIP Transformer	0.66	0.54	0.43	0.32	1.09	0.51	0.38
ViT and RoBERTa	0.74	0.63	0.55	0.46	1.80	0.68	0.56
ViT+ RoBERTa + CLIP	0.78	0.69	0.65	0.58	1.83	0.73	0.62
Tri-FusionNet (Proposed)	0.893	0.821	0.794	0.725	1.88	0.78	0.689

overlap, as shown by its ROUGE-L score of 0.689 and METEOR score of 0.78. When compared to the ViT + RoBERTa + CLIP model, which achieves scores of 0.78 for METEOR, 0.69 for ROUGE-L, 0.65 for BLEU-4, 0.58 for BLEU-3, 1.83 for CIDEr, 0.73 for BLEU-2, and 0.62 for BLEU-1, Tri-FusionNet’s performance highlights the effectiveness of its integrated attention mechanisms. The dual-attention mechanism proves especially useful, while the Vanilla ViT model demonstrates the strength of vision transformers. The CLIP Transformer outperforms the RoBERTa Transformer, despite the latter’s slight under-performance.

Table III displays a comprehensive analysis of the results obtained from the Flickr8k dataset in the context of the proposed work. It presents various evaluation metrics for different models applied to the input image. The Flickr30k

TABLE III
PERFORMANCE METRICS OF IMAGE DESCRIPTION GENERATION MODELS
IN THE FLICKR30K DATASET

Model	B-1	B-2	B-3	B-4	C	M	R-L
CNN-RNN Model	0.45	0.35	0.30	0.20	0.900	0.231	0.197
CNN-LSTM Model	0.43	0.32	0.25	0.18	0.901	0.28	0.25
ViT with Attention	0.47	0.33	0.23	0.17	0.907	0.34	0.331
ViT with Dual Attention	0.43	0.36	0.275	0.242	1.02	0.373	0.21
Vanilla ViT	0.682	0.513	0.420	0.382	0.355	0.412	0.353
ViT Only	0.614	0.586	0.542	0.443	0.855	0.544	0.393
RoBERTa Transformer	0.653	0.589	0.431	0.367	1.14	0.512	0.460
CLIP Transformer	0.516	0.424	0.343	0.232	1.256	0.534	0.489
ViT and RoBERTa	0.724	0.613	0.455	0.346	1.250	0.368	0.256
ViT+ RoBERTa + CLIP	0.741	0.621	0.573	0.428	1.092	0.389	0.432
Tri-FusionNet (Proposed)	0.767	0.654	0.647	0.456	1.679	0.478	0.567

dataset is used to evaluate several image description generation models, including ViT with RoBERTa, CNN-LSTM, Vanilla ViT, ViT with Attention, ViT with Dual Attention, ViT only, and RoBERTa Transformer. Despite its simplicity, the CNN-RNN Model provides competitive metrics and BLEU scores (0.20 to 0.45) as a baseline. The CNN-LSTM Model shows minor improvements, particularly in METEOR and ROUGE-L ratings. As demonstrated by higher METEOR, ROUGE-L, and BLEU-1 to BLEU-3 scores, the ViT with Attention and ViT with Dual Attention models benefit from attention mechanisms that improve language detail capture. While the RoBERTa Transformer performs exceptionally well in BLEU-2 and BLEU-3, the Vanilla ViT variant also performs robustly. The ViT + RoBERTa + CLIP model achieves scores of 0.741

for METEOR, 0.621 for ROUGE-L, 0.573 for BLEU-4, 0.428 for BLEU-3, 1.092 for CIDEr, 0.389 for BLEU-2, and 0.432 for BLEU-1. The Tri-FusionNet model produces accurate and varied visual descriptions, outperforming other models across BLEU-1 to BLEU-4 and achieving a BLEU-4 score of 0.456.

Table IV displays a comprehensive analysis of the results obtained from the Flickr8k dataset in the context of the proposed work. It presents various evaluation metrics for different models applied to the input image. Using CNN-LSTM and

TABLE IV
PERFORMANCE METRICS OF IMAGE DESCRIPTION GENERATION MODELS
IN THE FLICKR8K DATASET

Model	B-1	B-2	B-3	B-4	C	M	R-L
CNN-RNN Model	0.467	0.435	0.370	0.323	0.670	0.131	0.137
CNN-LSTM Model	0.433	0.232	0.225	0.118	0.301	0.128	0.235
ViT with Attention	0.547	0.343	0.323	0.217	0.607	0.234	0.131
ViT with Dual Attention	0.543	0.436	0.344	0.246	1.002	0.253	0.121
Vanilla ViT	0.632	0.511	0.320	0.242	0.255	0.316	0.153
ViT Only	0.542	0.466	0.342	0.266	0.675	0.344	0.343
RoBERTa Transformer	0.553	0.459	0.413	0.337	0.983	0.312	0.156
CLIP Transformer	0.525	0.324	0.244	0.132	1.065	0.234	0.289
ViT and RoBERTa	0.745	0.513	0.456	0.312	1.189	0.298	0.457
ViT+ RoBERTa + CLIP	0.756	0.652	0.518	0.460	1.231	0.321	0.528
Tri-FusionNet (Proposed)	0.784	0.678	0.538	0.479	1.381	0.389	0.654

CNN-RNN as baseline models, the Flickr8k dataset compares several image description models. While Vanilla ViT performs well in BLEU-1 to BLEU-2, attention mechanisms in ViT with Attention and ViT with Dual Attention models enhance visual descriptions. In BLEU-3 and CIDEr, ViT only, the RoBERTa Transformer outperforms the CLIP Transformer, which lags slightly behind. The ViT + RoBERTa + CLIP model achieves scores of 0.756 for METEOR, 0.652 for ROUGE-L, 0.518 for BLEU-4, 0.460 for BLEU-3, 1.231 for CIDEr, 0.321 for BLEU-2, and 0.528 for BLEU-1. ViT and RoBERTa work together to create a balanced model. Nonetheless, the suggested Tri-FusionNet surpasses all other models, attaining the highest ratings in CIDEr, ROUGE-L, and BLEU-1 to BLEU-4 measures, demonstrating its efficiency in producing precise and diverse image descriptions.

By combining language and vision transformer components, the Tri-FusionNet consistently outperforms other models in the MSCOCO, Flickr30k and Flickr8k datasets, demonstrating its superior architecture for image description generation and producing better image descriptions. It also yields higher scores in BLEU-1 to BLEU-4 metrics and CIDEr, ROUGE-L and other metrics.

B. Results and Analysis:

The approach was evaluated on three benchmark dataset: MSCOCO, Flickr30k and Flickr8k for the proposed architecture. The following Table V represents the results obtained for the MSCOCO dataset.

Using four sets of test images from the MSCOCO dataset, the table presents a thorough comparison of ground-truth descriptions and predicted descriptions generated by a model. This is an effective way of assessing and determining how well the model can provide meaningful and accurate descriptions of images.

TABLE V
QUANTITATIVE RESULTS OBTAINED ON MSCOCO DATASET

Test Image	Ground Truth	Predicted Description
	Two men playing frisbee on grass surrounded by trees.	Two men playing frisbee on grass.
	Trains on railway tracks, with trees and blue sky.	Trains on tracks with trees.
	Vegetables including carrot, radish and turnip on a table.	Green and red vegetables on a table.
	A red bus in front of a white building with blue sky.	A white building with blue sky.

TABLE VI
QUANTITATIVE RESULTS OBTAINED ON FLICKR30K DATASET

	
Ground Truth Descriptions	<ol style="list-style-type: none"> 1. A white woman standing in a grocery store not-so-candidly posing for the camera while examining the items on a shelf 2. The lady with the shopping cart is surrounded by toys galore and various children's bicycles. 3. A woman in a green winter coat stands with a cart in the middle of a department store aisle 4. a woman in a green jacket is in the toy aisle with a shopping cart and her purse 5. The woman in the green coat is pushing a cart through the toy aisle
Predicted Description	A woman in a green coat shops in the toy aisle with a cart.
	
Ground Truth Descriptions	<ol style="list-style-type: none"> 1. A gray bird stands majestically on a beach while waves roll in. 2. A white crane stands tall as it looks out upon the ocean. 3. A tall bird is standing on the sand beside the ocean. 4. A large bird stands in the water on the beach. 5. A water bird standing at the ocean's edge.
Predicted Description	A bird stands tall on the beach.
	
Ground Truth Descriptions	<ol style="list-style-type: none"> 1. Six men are sitting or laying on a patch of earth in a wooded area. 2. A group of workers sitting in a field take a break from work. 3. A group of men are sitting in the farm fields taking a break. 4. Six men sit in a field of crops containing wooden crates. 5. Pickers working out on a farm
Predicted Description	Six men take a break in a field.
	
Ground Truth Descriptions	<ol style="list-style-type: none"> 1. A group of people stares at a wall that is filled with drawings in a building. 2. There are 5 people here looking at some pictures on the wall. 3. Five people are taking in an exhibit of Japanese art. 4. People watching at the arts in exhibition. 5. Five people looking at artwork.
Predicted Description	Five people looking art in a building.

Table VI aims to showcase how well the model aligns for Flickr30k dataset. Four sets of test images are listed in the table, together with the accompanying ground truth descriptions and the model's predicted descriptions for each. This table is as an assessment tool, demonstrating the model's capacity to produce accurate and relevant descriptions for a range of images found in the Flickr30k dataset.

Table VII is designed to demonstrate the alignment of the model with the actual content of the images, as indicated by the provided ground truth descriptions for the Flickr8k dataset. Four sets of test images are included in the table, each with the corresponding ground truth descriptions and the predicted descriptions from the model. This table serves as a means of assessment, showcasing the model's capacity to provide accurate and perceptive descriptions for a range of images from the Flickr8k dataset.

TABLE VII
QUANTITATIVE RESULTS OBTAINED ON FLICKR8K DATASET

	
Ground Truth Descriptions	<ol style="list-style-type: none"> 1. A winter landscape with four people walking in the snow. 2. Beautiful snowy landscape with people treading through the snow. 3. Cross-country skiers are traveling towards the mountains at sunset. 4. Four people walking across thick snow during a sunset. 5. The sun is almost behind the snowy mountains.
Predicted Description	Four people walk through a snowy mountain.
	
Ground Truth Descriptions	<ol style="list-style-type: none"> 1. "a crowd wearing red , cheers on the red football team." 2. Football players in red congratulate each other as crowds in red cheer behind. 3. The Oklahoma Sooners football team discuss their game while fans cheer. 4. Two football players talk during a game. 5. Two Oklahoma Sooner football players talk on the sideline.
Predicted Description	A crowd in red cheers on the football team.
	
Ground Truth Descriptions	<ol style="list-style-type: none"> 1. The two small dogs run through the grass. 2. Two fluffy white dogs running in green grass. 3. Two small dogs run through the grass. 4. Two small dogs that look almost identical are playing in the grass. 5. Two yellow dogs run together in green grass.
Predicted Description	Two small dogs run through the green grass.

When compared to reference descriptions, the model produces predicted descriptions during the training and evaluation phases. The model's efficacy in capturing visual semantics and context is evaluated by comparing the predicted and real descriptions using metrics such as BLEU 1-4, CIDEr, METEOR and ROUGE-L. Table VIII provides an overview of a framework that has been suggested for the development of image descriptions from the three datasets.

TABLE VIII
OVERALL RESULTS OBTAINED FROM THE PROPOSED MODEL

Dataset	B-1	B-2	B-3	B-4	C	M	R-L
MSCOCO	0.893	0.821	0.794	0.725	1.88	0.78	0.689
Flickr30k	0.767	0.654	0.647	0.456	1.679	0.478	0.567
Flickr8k	0.784	0.678	0.538	0.479	1.381	0.389	0.654

The performance metrics of the proposed model are shown in the table for the MSCOCO, Flickr30k and Flickr8k datasets. These metrics include BLEU-1 to BLEU-4, CIDEr, METEOR and ROUGE-L scores. The suggested framework obtained BLEU scores for MSCOCO of 0.893 (B-1), 0.821 (B-2), 0.794 (B-3) and 0.725 (B-4) and for CIDEr, METEOR and ROUGE-L, 1.483, 0.358 and 0.789, respectively. With BLEU scores ranging from 0.767 (B-1) to 0.456 (B-4), bolstered by a CIDEr score of 1.679 and METEOR (0.478) and ROUGE-L (0.567) ratings suggesting sufficient matching and overlap, competitive performance was observed on the Flickr30k dataset. A CIDEr score of 1.381, favorable matches, and overlap was shown by BLEU scores on the Flickr8k dataset, which varied from 0.784 (B-1) to 0.479 (B-4). METEOR (0.389) and ROUGE-L (0.654)

scores also showed favorable matches and overlap. Across a range of benchmark datasets, the proposed approach performs well overall in producing image descriptions. The graphical depiction of the outcomes is shown in Figure 3. These scores

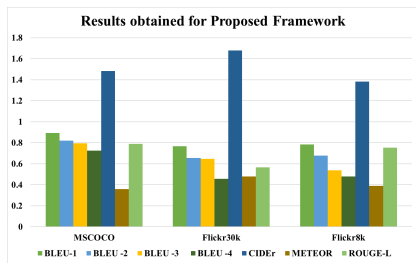


Fig. 3. Graphical representation of the results obtained from the datasets for the proposed Tri-FusionNet framework.

serve as evaluations of the model’s performance in generating descriptions that align well with the reference descriptions. Higher scores indicate a higher degree of similarity and quality in the generated descriptions.

Table IX presents a qualitative comparison between the ground truth descriptions and the descriptions generated by the proposed model, highlighting successful and unsuccessful predictions and error analysis.

TABLE IX
QUALITATIVE ANALYSIS OF GENERATED IMAGE DESCRIPTIONS

Test Image	Ground Truth Description	Generated Description	Remarks/Error Analysis
	A white dog is holding a purple frisbee in its mouth on the green grass.	White dog holding purple frisbee on grass.	Success: Correct identification of objects and actions.
	A gold and black motorcycle parked on a paved surface road.	A car parked on road.	Failure: Incorrect object recognition.
	Three ducks stand by a calm pond with a wooden fence in front of them.	Three ducks stand by pond.	Success: Correct identification of objects and actions.
	A red and white vintage plane on display in a museum.	Spaceship preparing to launch.	Failure: Incorrect object recognition.

The following table compares the generated descriptions of four sample images with ground truth annotations to evaluate the performance of an image captioning model. Successful examples include correctly identifying “three ducks on a peaceful pond” and “a white dog clutching a purple frisbee on grass.” These cases demonstrate the model’s ability to recognize objects and actions in straightforward scenarios. However, the model exhibits notable failures, such as mistaking a gold and black motorcycle for “a car parked on a road” and, in row 4, misidentifying a red and white vintage plane as “a spaceship preparing to launch.” These errors highlight the model’s difficulty in accurately identifying complex objects or understanding the context of the scene. This analysis provides valuable insights into the model’s strengths in simple situations and its limitations when faced with more intricate

or ambiguous visuals, offering guidance for improving the model’s training and recognition capabilities.

C. Comparison with Other State-of-the-art Methods:

A comprehensive generalisation analysis highlights the performance of the proposed model outside of the training set by assessing its capacity to produce image descriptions over a wide range of visual domains and datasets. A comparison study of image description generation models using the MSCOCO dataset is presented in Table X, which evaluates model performance using metrics such as BLEU, METEOR, CIDEr and Rouge-L.

TABLE X
COMPARATIVE ANALYSIS OF IMAGE DESCRIPTION GENERATION MODELS ON MSCOCO DATASET

Model	BLEU	METEOR	CIDEr	Rouge-L
Topic-based multi-channel attention (TMA) model [21]	0.658	-	0.800	0.534
Transformer based local graph semantic attention (TLGSA) [22]	0.724	-	1.003	0.534
Dynamic-balanced double-attention [23]	0.741	0.254	1.107	0.537
Meshed Transformer [7]	0.816	0.294	1.293	0.592
Global Enhanced Transformer [24]	0.816	0.284	1.301	0.591
Multimodal Transformer [8]	0.817	0.294	1.30	0.596
S^2 Transformer [12]	0.811	0.296	1.335	0.591
PMA-Net [15]	0.847	0.305	1.414	0.613
HAHV [16]	0.810	0.302	1.415	-
SPT Transformer [18]	0.812	0.296	1.344	0.592
Geometry attention transformer [25]	0.811	0.384	1.27	0.591
Vision-enhanced and Consensus-aware Transformer [26]	0.822	0.296	1.345	0.596
X-transformer + Faster RCNN [27]	0.821	0.296	1.334	0.598
Local-global guidance for transformer [28]	0.861	0.392	1.329	0.651
SAMT [11]	0.774	0.284	1.205	0.572
Tri-FusionNet (Proposed)	0.893	0.780	1.880	0.689

The performance of different models on the MSCOCO dataset indicates strong progress in image description generation. Models like Meshed Transformer [7], Global Enhanced Transformer [24], and Multimodal Transformer [8] show strong overall performance in terms of high scores obtained in BLEU, METEOR, CIDEr, and Rouge-L metrics. In contrast, models like Topic-based multi-channel attention (TMA) [21], Transformer-based local graph semantic attention (TLGSA) [22], and Dynamic-balanced double-attention [23] have relatively weaker performance, especially in terms of BLEU and CIDEr scores. Geometry Attention Transformer [25] and S^2 Transformer [12] obtain the best CIDEr scores, while Local-global guidance for transformer [28] reaches the best Rouge-L score of 0.651. Among the best-performing models, PMA-Net [15] and HAAV [16] obtain CIDEr scores higher than 1.4. In addition, PMA-Net obtains the best BLEU score of 0.847 among all the models. However, Tri-FusionNet breaks all other records as the new baseline, obtaining state-of-the-art performance scores for both BLEU 0.893, METEOR 0.780, CIDEr 1.880, and also Rouge-L with a 0.689 score in all the tested metrics, which highlights its capacity in producing better descriptions with semantic accuracy of an image for all the existing models.

To further validate the performance of the proposed Tri-FusionNet model, we evaluated it on the online MSCOCO test server, which is widely used as a benchmark for image description generation. The comparative results are presented in Table XI, highlighting the superior performance of Tri-

FusionNet in all the metrics, demonstrating its efficiency in generating contextually rich and accurate image descriptions.

TABLE XI
COMPARATIVE ANALYSIS OF IMAGE DESCRIPTION GENERATION MODELS ON ONLINE MSCOCO TEST SERVER

Model	BLEU	METEOR	Rouge-L	CIDEr
NIC [19]	0.714	0.302	0.521	0.945
m-RNN [29]	0.753	0.301	0.593	0.926
ReviewNet [30]	0.810	0.301	0.609	0.967
SCN [31]	0.828	0.309	0.619	1.013
Adaptive [32]	0.834	0.311	0.628	1.051
Att2all [33]	0.859	0.312	0.635	1.157
GateCap [34]	0.863	0.319	0.644	1.190
LSTM-A [35]	0.862	0.312	0.635	1.170
Up-Down [36]	0.877	0.322	0.648	1.192
RFNet [37]	0.877	0.327	0.657	1.240
GCN-LSTM [38]	-	0.330	0.660	1.259
SGAE [39]	0.882	0.327	0.661	1.252
AoANet [40]	0.880	0.338	0.667	1.282
Tri-FusionNet (Proposed)	0.885	0.750	0.678	1.580

Table XII compares various image description generation models using the Flickr30k dataset. The analysis includes metrics for evaluating the models' performance, such as BLEU, METEOR, CIDEr, and Rouge-L.

TABLE XII
COMPARATIVE ANALYSIS OF IMAGE DESCRIPTION GENERATION MODELS ON FLICKR30K DATASETS

Model	BLEU	METEOR	CIDEr	Rouge-L
Topic-based multi-channel attention (TMA) model [21]	0.650	-	0.334	0.436
Transformer based local graph semantic attention (TLGSA) [22]	0.643	-	0.450	0.489
Dynamic-balanced double-attention [23]	0.678	0.209	0.517	0.500
HAAV [16]	0.743	0.251	0.856	-
Multimodal Transformer [8]	0.744	0.236	-	-
Local-global guidance for transformer [28]	0.758	0.263	0.708	0.560
X-transformer + Faster RCNN [27]	0.753	0.253	0.707	0.543
Tri-FusionNet (Proposed)	0.767	0.478	1.679	0.567

Models like Transformer-based local graph semantic attention (TLGSA) [22], Topic-based multi-channel attention (TMA) [21], and Dynamic-balanced double-attention [23] show lower performance, particularly in BLEU and CIDEr, indicating limitations in generating high-quality descriptions. While the Multimodal Transformer [8] performs well in BLEU and METEOR, it lacks comprehensive metric coverage. Local-global guidance for Transformer [28] and X-transformer + Faster RCNN [27] demonstrate strong BLEU and CIDEr scores but fall slightly behind in Rouge-L. HAAV [16] achieves notable performance, especially with a CIDEr score of 0.856. However, the proposed Tri-FusionNet outperforms all models, achieving the highest scores across all metrics: 0.767 for BLEU, 0.478 for METEOR, 1.679 for CIDEr, and 0.567 for Rouge-L, establishing it as the most effective model for generating accurate and contextually rich descriptions on the Flickr30k dataset.

Table XIII presents a comparative analysis of various image description generation models on the Flickr8k dataset. It offers evaluation metrics for evaluating how well various models perform, including BLEU, METEOR, CIDEr and Rouge-L.

Models like TLGSA based on transformer [22], Vision encoder-decoder [41], Topic-based multi-channel attention [21], and Optimal transformers with beam search [42] have performance relatively lower and are bad at BLEU and CIDEr

TABLE XIII
COMPARATIVE ANALYSIS OF IMAGE DESCRIPTION GENERATION MODELS ON FLICKR8K DATASET

Model	BLEU	METEOR	CIDEr	Rouge-L
Topic-based multi-channel attention (TMA) model [21]	0.630	-	0.472	0.465
Transformer based local graph semantic attention (TLGSA) [22]	0.659	-	0.471	0.565
Vision encoder decoder [41]	0.395	0.177	0.380	0.297
Optimal transformers with Beam Search [42]	0.634	0.1987	0.520	-
SAMT [11]	0.682	0.212	-	0.448
Tri-FusionNet (Proposed)	0.784	0.389	1.381	0.654

score, due to the lesser ability for producing high quality and relevant descriptions. Specifically, even though SAMT [11] has scores of BLEU and METEOR comparatively better values, it also lacks other competitive values of CIDEr and Rouge-L. On the other hand, proposed Tri-FusionNet obtains excellent results with setting new state-of-the-art for all metrics: BLEU-0.784, METEOR-0.389, CIDEr-1.381, and Rouge-L - 0.654. Such results emphasize that the proposed Tri-FusionNet model is more likely to produce exceptional, meaningful, and expressive image descriptions compared to existing models for Flickr8k.

V. CONCLUSION AND FUTURE DIRECTION

In this paper, a new model, Tri-FusionNet, for generating image descriptions that combine the CLIP transformer, RoBERTa, and the Vision Transformer with dual-attention processes, was presented. The proposed model outperforms state-of-the-art models as a result of extensive trials on the MSCOCO, Flickr30k, and Flickr8k datasets. It achieved notable gains across important evaluation criteria, such as BLEU, METEOR, CIDEr, and ROUGE. The model is successful because it can capture both local and global image data, use the CLIP transformer to effectively align textual and visual modalities, and employ RoBERTa for improved language understanding. The suggested model has useful applications in real-time image captioning systems, including autonomous car systems for scene detection, assistive technologies for the blind, and content management systems for automatic image tagging. Deploying the model still presents difficulties, though, such as managing edge devices' demanding processing requirements, ensuring the system is resilient to threats and noisy inputs, and resolving ethical challenges like bias in generated captions. Furthermore, the model's performance may be impacted by the unpredictability introduced by real-world settings, such as occlusions, dim lighting, computational cost, and other social circumstances. To enable more extensive real-world applications, future research will concentrate on improving fine-tuning procedures, tackling deployment issues, and extending the model's capabilities through sophisticated multimodal fusion techniques.

Supplementary Material The supplementary material contains additional experimental details, architectures and algorithm of the proposed work. The file `supplementary.txt` is available alongside this manuscript in the submission system.

Acknowledgment The Malware and Cyber-Forensics Lab at

Delhi Technological University, New Delhi, India, is acknowledged by the authors for providing the resources required to complete the research.

Data Availability Statement All the dataset links are provided in the paper.

Conflict of Interest The authors declare that they have no conflict of interest.

REFERENCES

- [1] T. Ghandi, H. Pourreza, and H. Mahyar, "Deep learning approaches on image captioning: A review," *ACM Computing Surveys*, vol. 56, no. 3, pp. 1–39, 2023.
- [2] L. Agarwal and B. Verma, "From methods to datasets: A survey on image-caption generators," *Multimedia Tools and Applications*, vol. 83, no. 9, pp. 28 077–28 123, 2024.
- [3] K. Han, Y. Wang, H. Chen, X. Chen, J. Guo, Z. Liu, Y. Tang, A. Xiao, C. Xu, Y. Xu *et al.*, "A survey on vision transformer," *IEEE transactions on pattern analysis and machine intelligence*, vol. 45, no. 1, pp. 87–110, 2022.
- [4] V. Atliha and D. Šešok, "Text augmentation using bert for image captioning," *Applied Sciences*, vol. 10, no. 17, p. 5978, 2020.
- [5] X. Pan, T. Ye, D. Han, S. Song, and G. Huang, "Contrastive language-image pre-training with knowledge graphs," *Advances in Neural Information Processing Systems*, vol. 35, pp. 22 895–22 910, 2022.
- [6] G. Li, L. Zhu, P. Liu, and Y. Yang, "Entangled transformer for image captioning," in *Proceedings of the IEEE/CVF international conference on computer vision*, 2019, pp. 8928–8937.
- [7] M. Cornia, M. Stefanini, L. Baraldi, and R. Cucchiara, "Meshed-memory transformer for image captioning," in *Proceedings of the IEEE/CVF conference on computer vision and pattern recognition*, 2020, pp. 10 578–10 587.
- [8] J. Yu, J. Li, Z. Yu, and Q. Huang, "Multimodal transformer with multi-view visual representation for image captioning," *IEEE transactions on circuits and systems for video technology*, vol. 30, no. 12, pp. 4467–4480, 2019.
- [9] A. Radford, J. W. Kim, C. Hallacy, A. Ramesh, G. Goh, S. Agarwal, G. Sastry, A. Askell, P. Mishkin, J. Clark *et al.*, "Learning transferable visual models from natural language supervision," in *International conference on machine learning*. PMLR, 2021, pp. 8748–8763.
- [10] J. Chen, D. Zhu, X. Shen, X. Li, Z. Liu, P. Zhang, R. Krishnamoorthi, V. Chandra, Y. Xiong, and M. Elhoseiny, "Minigt-v2: large language model as a unified interface for vision-language multi-task learning," *arXiv preprint arXiv:2310.09478*, 2023.
- [11] X. Yang, Y. Yang, S. Ma, Z. Li, W. Dong, and M. Woźniak, "Samt-generator: A second-attention for image captioning based on multi-stage transformer network," *Neurocomputing*, vol. 593, p. 127823, 2024.
- [12] P. Zeng, H. Zhang, J. Song, and L. Gao, "S2 transformer for image captioning," in *IJCAI*, 2022, pp. 1608–1614.
- [13] X. Yang, Y. Yang, J. Wu, W. Sun, S. Ma, and Z. Hou, "Ca-captioner: A novel concentrated attention for image captioning," *Expert Systems with Applications*, vol. 250, p. 123847, 2024.
- [14] H. Parvin, A. R. Naghsh-Nilchi, and H. M. Mohammadi, "Image captioning using transformer-based double attention network," *Engineering Applications of Artificial Intelligence*, vol. 125, p. 106545, 2023.
- [15] M. Barraco, S. Sarto, M. Cornia, L. Baraldi, and R. Cucchiara, "With a little help from your own past: Prototypical memory networks for image captioning," in *Proceedings of the IEEE/CVF International Conference on Computer Vision*, 2023, pp. 3021–3031.
- [16] C.-W. Kuo and Z. Kira, "Haav: Hierarchical aggregation of augmented views for image captioning," in *Proceedings of the IEEE/CVF conference on computer vision and pattern recognition*, 2023, pp. 11 039–11 049.
- [17] T. Yao, Y. Li, Y. Pan, Y. Wang, X.-P. Zhang, and T. Mei, "Dual vision transformer," *IEEE transactions on pattern analysis and machine intelligence*, 2023.
- [18] H. Zhang, P. Zeng, L. Gao, X. Lyu, J. Song, and H. T. Shen, "Spt: Spatial pyramid transformer for image captioning," *IEEE Transactions on Circuits and Systems for Video Technology*, 2023.
- [19] O. Vinyals, A. Toshev, S. Bengio, and D. Erhan, "Show and tell: A neural image caption generator," in *Proceedings of the IEEE conference on computer vision and pattern recognition*, 2015, pp. 3156–3164.
- [20] J. Li, D. Li, C. Xiong, and S. Hoi, "Blip: Bootstrapping language-image pre-training for unified vision-language understanding and generation," in *International conference on machine learning*. PMLR, 2022, pp. 12 888–12 900.
- [21] K. Qian and L. Tian, "A topic-based multi-channel attention model under hybrid mode for image caption," *Neural Computing and Applications*, vol. 34, no. 3, pp. 2207–2216, 2022.
- [22] K. Qian, Y. Pan, H. Xu, and L. Tian, "Transformer model incorporating local graph semantic attention for image caption," *The Visual Computer*, pp. 1–12, 2023.
- [23] C. Wang and X. Gu, "Dynamic-balanced double-attention fusion for image captioning," *Engineering Applications of Artificial Intelligence*, vol. 114, p. 105194, 2022.
- [24] J. Ji, Y. Luo, X. Sun, F. Chen, G. Luo, Y. Wu, Y. Gao, and R. Ji, "Improving image captioning by leveraging intra-and inter-layer global representation in transformer network," in *Proceedings of the AAAI conference on artificial intelligence*, vol. 35, no. 2, 2021, pp. 1655–1663.
- [25] C. Wang, Y. Shen, and L. Ji, "Geometry attention transformer with position-aware lstms for image captioning," *Expert systems with applications*, vol. 201, p. 117174, 2022.
- [26] S. Cao, G. An, Z. Zheng, and Z. Wang, "Vision-enhanced and consensus-aware transformer for image captioning," *IEEE Transactions on Circuits and Systems for Video Technology*, vol. 32, no. 10, pp. 7005–7018, 2022.
- [27] L. Lou, K. Lu, and J. Xue, "A novel cross-fusion method of different types of features for image captioning," in *2023 International Joint Conference on Neural Networks (IJCNN)*. IEEE, 2023, pp. 1–8.
- [28] H. Parvin, A. R. Naghsh-Nilchi, and H. M. Mohammadi, "Transformer-based local-global guidance for image captioning," *Expert Systems with Applications*, vol. 223, p. 119774, 2023.
- [29] J. Mao, "Deep captioning with multimodal recurrent neural networks (m-rnn)," *arXiv preprint arXiv:1412.6632*, 2014.
- [30] Z. Yang, Y. Yuan, Y. Wu, W. W. Cohen, and R. R. Salakhutdinov, "Review networks for caption generation," *Advances in neural information processing systems*, vol. 29, 2016.
- [31] Z. Gan, C. Gan, X. He, Y. Pu, K. Tran, J. Gao, L. Carin, and L. Deng, "Semantic compositional networks for visual captioning," in *Proceedings of the IEEE conference on computer vision and pattern recognition*, 2017, pp. 5630–5639.
- [32] J. Lu, C. Xiong, D. Parikh, and R. Socher, "Knowing when to look: Adaptive attention via a visual sentinel for image captioning," in *Proceedings of the IEEE conference on computer vision and pattern recognition*, 2017, pp. 375–383.
- [33] S. J. Rennie, E. Marcheret, Y. Mroueh, J. Ross, and V. Goel, "Self-critical sequence training for image captioning," in *Proceedings of the IEEE conference on computer vision and pattern recognition*, 2017, pp. 7008–7024.
- [34] S. Wang, L. Lan, X. Zhang, and Z. Luo, "Gatecap: Gated spatial and semantic attention model for image captioning," *Multimedia Tools and Applications*, vol. 79, pp. 11 531–11 549, 2020.
- [35] T. Yao, Y. Pan, Y. Li, Z. Qiu, and T. Mei, "Boosting image captioning with attributes," in *Proceedings of the IEEE international conference on computer vision*, 2017, pp. 4894–4902.
- [36] P. Anderson, X. He, C. Buehler, D. Teney, M. Johnson, S. Gould, and L. Zhang, "Bottom-up and top-down attention for image captioning and visual question answering," in *Proceedings of the IEEE conference on computer vision and pattern recognition*, 2018, pp. 6077–6086.
- [37] W. Jiang, L. Ma, Y.-G. Jiang, W. Liu, and T. Zhang, "Recurrent fusion network for image captioning," in *Proceedings of the European conference on computer vision (ECCV)*, 2018, pp. 499–515.
- [38] T. Yao, Y. Pan, Y. Li, and T. Mei, "Exploring visual relationship for image captioning," in *Proceedings of the European conference on computer vision (ECCV)*, 2018, pp. 684–699.
- [39] X. Yang, K. Tang, H. Zhang, and J. Cai, "Auto-encoding scene graphs for image captioning," in *Proceedings of the IEEE/CVF conference on computer vision and pattern recognition*, 2019, pp. 10 685–10 694.
- [40] L. Huang, W. Wang, J. Chen, and X.-Y. Wei, "Attention on attention for image captioning," in *Proceedings of the IEEE/CVF international conference on computer vision*, 2019, pp. 4634–4643.
- [41] A. Abdelaal, N. F. ELshafey, N. W. Abdalah, N. H. Shaaban, S. A. Okasha, T. Yasser, M. Fathi, K. M. Fouad, and I. Abdelbaky, "Image captioning using vision encoder decoder model," in *2024 International Conference on Machine Intelligence and Smart Innovation (ICMISI)*. IEEE, 2024, pp. 101–106.
- [42] A. Shetty, Y. Kale, Y. Patil, R. Patil, and S. Sharma, "Optimal transformers based image captioning using beam search," *Multimedia Tools and Applications*, vol. 83, no. 16, pp. 47 963–47 977, 2024.